Scientific Research Publishing

Materials Sciences and Applications, 2024, 15, 213-227
https://www.scirp.org/journal/msa
ISSN Online: 2153-1188
ISSN Print: 2153-117X

Mechanical and Electrical Properties of Some Sn-Zn Based Lead-Free Quinary Alloys

Shihab Uddin[1], Md. Abdul Gafur[2*], Suraya Sabrin Soshi[3], Mohammad Obaidur Rahman[1]

[1]Department of Physics, Jahangirnagar University, Savar, Dhaka, Bangladesh
[2]Pilot Plant and Process Development Centre, Dhaka, Bangladesh
[3]Department of Mechanical Engineering, Ahsanullah University of Science and Technology, Tejgaon, Dhaka, Bangladesh
Email: *d_r_magafur@yahoo.com

How to cite this paper: Uddin, S., Gafur, M.A., Soshi, S.S. and Rahman, M.O. (2024) Mechanical and Electrical Properties of Some Sn-Zn Based Lead-Free Quinary Alloys. *Materials Sciences and Applications*, **15**, 213-227.
https://doi.org/10.4236/msa.2024.157015

Received: April 24, 2024
Accepted: July 19, 2024
Published: July 22, 2024

Abstract

Although there are many lead-free soldering alloys on the market, none of them have ideal qualities. The researchers are combining binary alloys with a variety of additional materials to create the soldering alloys' features. The eutectic Sn-9Zn alloy is among them. This paper investigated the mechanical and electrical properties of Sn-9Zn-x (Ag, Cu, Sb); {x = 0.2, 0.4, and 0.6} lead-free solder alloys. The mechanical properties such as elastic modulus, ultimate tensile strength (UTS), yield strength (YS), and ductility were examined at the strain rates in a range from 4.17×10^{-3} s^{-1} to 208.5×10^{-3} s^{-1} at room temperature. It is found that increasing the content of the alloying elements and strain rate increases the elastic modulus, ultimate tensile strength, and yield strength while the ductility decreases. The electrical conductivity of the alloys is found to be a little smaller than that of the Sn-9Zn eutectic alloy.

Keywords

Lead-Free Solder, Strain Rate, Ultimate Tensile Strength, Ductility, Electrical Conductivity

1. Introduction

Due to their superior mechanical qualities, lower melting point (183°C), and wetting propensity, the eutectic composition of Sn-Pb solder alloys has gained popularity in recent decades [1] [2]. It is suitable for PCB laminate materials and does not alter the microstructure of the base metal because of its lower melting temperature. Lead toxicity is well known to be hazardous to the environment and public health, and its usage is prohibited [3]-[10]. Direct exposure to lead and lead-containing elements in paints, fuels, and pipes has been reduced be-

cause of the ban on lead and lead-containing products in these uses. The electronics industries are apprehensive about substituting conventional lead-based solders with lead-free solder alloys because of environmental and health hazards, legal restrictions, environmental laws like the Restriction of the Use of Hazardous Substances (RoHS) and Waste Electrical and Electronic Equipment (WEEE) in the European Union (EU), South Korea, Türkiye, China, Japan, and the United States, and marketing forces both domestically and internationally [11]-[18]. Several indices, including melting temperature, mechanical characteristics, wetting qualities, electrochemical behaviors, practicality, and cost factor, must be taken into account while developing and researching an alternative solder alloy [19]-[21]. Because of their superior performance, dependability, affordability, and resource availability, researchers are focusing their attention primarily on Sn-Ag and Sn-Zn alloys. Sn-Zn solders have several advantages over Sn-Ag solders, including a lower melting point, enough mechanical strength, affordability, and accessibility. Thus, there's a fantastic chance to consider Sn-Zn solder [22]-[24].

Because Sn-Zn-based solder alloys have superior mechanical qualities compared to lead-based solders, they might be a good substitute. With a lower melting point of 198˚C, the mechanical properties of the Sn-9Zn eutectic alloy are superior to those of conventional solder alloys [25] [26]. Leaded solder alloys are expected to be replaced by the Sn-9Zn eutectic alloy due to its many benefits. Sn-9Zn eutectic alloy is considerably more suitable than Sn-Pb eutectic solder, but it also has significant drawbacks, including poorer oxidation resistance, reduced wettability, and worse corrosion behavior [27] [28]. These undesirable features prevent the Sn-9Zn eutectic alloy from replacing Sn-Pb solders [29] [30]. To address the current shortage in the Sn-9Zn eutectic alloy, some researchers have attempted to supplement the Sn-Zn binary system with one or more elements, such as P, Nd, Ag, Cr, Ni, Ga, Sb, Bi-In, Al and Cu, Bi, Ga-Al-Ag-Ce, Ga-Ag/Ga-Al-Ag, and Ga-Nd [31]-[42]. The application of the Sn-9Zn eutectic alloy is growing every day, despite its numerous drawbacks.

Therefore, more research is needed to look at the material's characteristics, including its melting point, mechanical strength, ductility, electrochemical behavior, thermal fatigue, solderability, electrical properties, and creep resistance, among others. The mechanical, and electrical properties of a solder alloy are very significant, as mechanical properties determine the thermal fatigue and fracture and electrical properties determine the electrical conductivity of the solder joint. Therefore, it is necessary to investigate the solder's mechanical (hardness, tensile strength, yield strength, ductility, and elastic modulus) and electrical properties. In this study, the effect of simultaneous addition of different contents of Ag, Cu, and Sb on the mechanical and electrical properties of Sn-9Zn eutectic solder alloy was investigated. The mechanical properties such as elastic modulus, ultimate tensile strength (UTS), yield stress (YS), and ductility (% elongation) were compared for the solder alloys Sn-9Zn-0.2Ag-0.2Cu-0.2Sb,

Sn-9Zn-0.4Ag-0.4Cu-0.4Sb, and Sn-9Zn-0.6Ag-0.6Cu-0.6Sb at the strain rates in a range from 4.17×10^{-3} s^{-1} to 208.5×10^{-3} s^{-1} at room temperature.

2. Experimental Procedure

2.1. Preparation of the Samples

Raw materials for preparing the alloys, pure tin (99.5 wt%), pure zinc (99.5 wt%), pure copper (99.5 wt%), pure silver (99.5 wt%), and pure antimony (99.5 wt%) are available in the local market. At first, the master alloy Sn–10Cu is prepared. The calculated amount of tin and copper is weighted. Subsequently, copper is put in a graphite crucible and heated to 11,00˚C in an electric melting furnace for ten minutes. Tin is added to the copper after it has melted, and the temperature stays the same until the melting is complete. The liquid solder alloy was cast in a 250 mm × 10 mm × 10 mm cast iron mold that had been warmed to 300˚C before cooling in the air. Every solder is poured into the form of an ingot that is rectangular. The melt was stirred to achieve homogeneity prior to casting. To eliminate micro-segregation effects, the as-cast alloys are annealed for 60 minutes at 150˚C, then cooled in a furnace. To prepare the quinary alloys, the calculated amounts of master alloy, tin, zinc, silver, and antimony are taken. Ten minutes at 430˚C in a muffle furnace are used to melt the master alloy, tin, and zinc contained in a clay graphite crucible. Subsequently, the crucible is filled with additional alloying components, such as antimony and silver, and left to reach 500˚C for 20 minutes. A 250 mm × 10 mm × 10 mm cast iron mold that had been preheated to 300˚C was used to metal cast the liquid solder alloy, which was then allowed to cool. Before casting, the melt was stirred to make it homogeneous. Following a 60-minute annealing process at 150˚C, the as-cast alloys are cooled in the furnace. As-cast alloys were then sectioned and polished to prepare for characterization.

2.2. Microhardness Test

Microhardness tests were conducted using a Vickers microhardness tester. For microhardness testing, a flat and smooth surface is necessary. To obtain a smooth and flat surface for hardness tests, proper grinding and polishing are necessary. Therefore, samples were appropriately polished before indentation. To create a clear indentation for the microhardness test, the polished samples were inserted into the machine. The samples were studied for microhardness with the HMV-2T, Shimadzu Co., Japan, Vickers Microhardness Tester. The applied load was 50 g for 10 seconds. Each alloy was subjected to five room-temperature indentations to determine the average value. The standard deviation was also calculated. The values of microhardness were calculated from the following equation:

$$\mathrm{HV} = 1.854\frac{F}{d^2} \tag{1}$$

where, HV = Vickers hardness Number, F = applied load measured in kilo-

gram-force, and d = arithmetic mean of the two diagonal lengths (mm) of indentation.

2.3. Tensile Tests

The tensile test is performed in a Universal Testing Machine (brand: Hounsfield, SR. No. H10KS-0572) at the cross-head speed of 2 mm/min, 10 mm/min, and 100 mm/min which is equal to the nominal strain rate of 4.17×10^{-3} s^{-1}, 20.85×10^{-3} s^{-1}, and 208.5×10^{-3} s^{-1}. Up until the specimen fails, the test is conducted at room temperature. Here are representative test curves for one sample of each alloy; test curves for the other samples, which showed comparable form and appearance, are not provided. The test is performed for the same three alloys, and the average of these results is taken as the test result for the corresponding alloy. The dimensions of the samples are gauge length 8 mm, thickness 2 mm, and width 3 mm as shown in Figure 1.

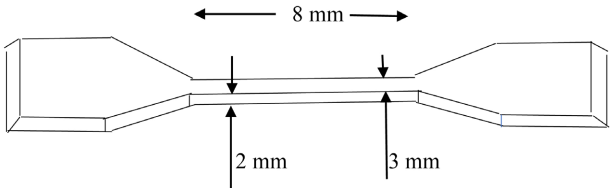

Figure 1. Dimensions of the tensile specimen.

2.4. Electrical Tests

A digital electrical conductivity meter (Technofour, type 979, India) is used to measure the electrical conductivity of the alloys in % I.A.C.S. (International Annealed Copper Standard). A hand-held probe is used to take the readings right away. Eddy currents at a set frequency are induced in the test portion when the probe is positioned on its flat surface. Specimens' electrical conductivity is directly correlated with the electrical impedance of the test probe, which is impacted by these currents [43]. With an accuracy of ±1% I.A.C.S., the conductivity of the test sample is expressed as a percentage on a digital display upon detection and processing of the change in probe impedance.

3. Results and Discussion

The chemical compositions of the alloys are measured with a BRUKER S1TITAN Handheld XRF Analyzer, shown in Table 1 (wt%).

Table 1. Chemical compositions of the quinary alloys (wt%).

Solder alloy	Sn	Zn	Ag	Cu	Sb
(A-1) Sn-9Zn-0.2Ag-0.2Cu-0.2Sb	90.194	9.212	0.191	0.215	0.188
(A-2) Sn-9Zn-0.4Ag-0.4Cu-0.4Sb	89.753	8.981	0.436	0.441	0.389
(A-3) Sn-9Zn-0.6Ag-0.6Cu-0.6Sb	88.927	9.242	0.608	0.632	0.591

3.1. Microstructural Analysis

The uniformity in the microstructure of a material has a great influence on its mechanical properties. Microscopic analysis of the prepared samples is carried out to know how the different phases are distributed in the alloys. The microstructure of the alloys is analyzed with a scanning electron microscope (Model: JOEL JSM-7600F). The SEM micrograph is presented in Figure 2. The microstructure of the alloys has a brighter area (β-Sn) and a darker area (IMC).

The intermetallic compound phases are distributed in the Sn matrix with irregular shapes. Due to the addition of different amounts of multi-alloying elements simultaneously, the Zn-rich phase disappears, and different complex-shaped intermetallic compounds form and disperse in the β-Sn matrix. XRD data indicates that as the amount of alloying element increases, the crystallite size increases, and the dislocation density decreases.

3.2. XRD Analysis

The X-ray diffractometry (XRD) patterns of the quinary alloys are shown in Figure 3. Analyzing the patterns, it is observed that all the alloys have Sn (tetragonal), $Sb_{30}Zn_{38.41}$ (hexagonal), and $Sb_{30}Zn_{38.45}$ (hexagonal) phases in common.

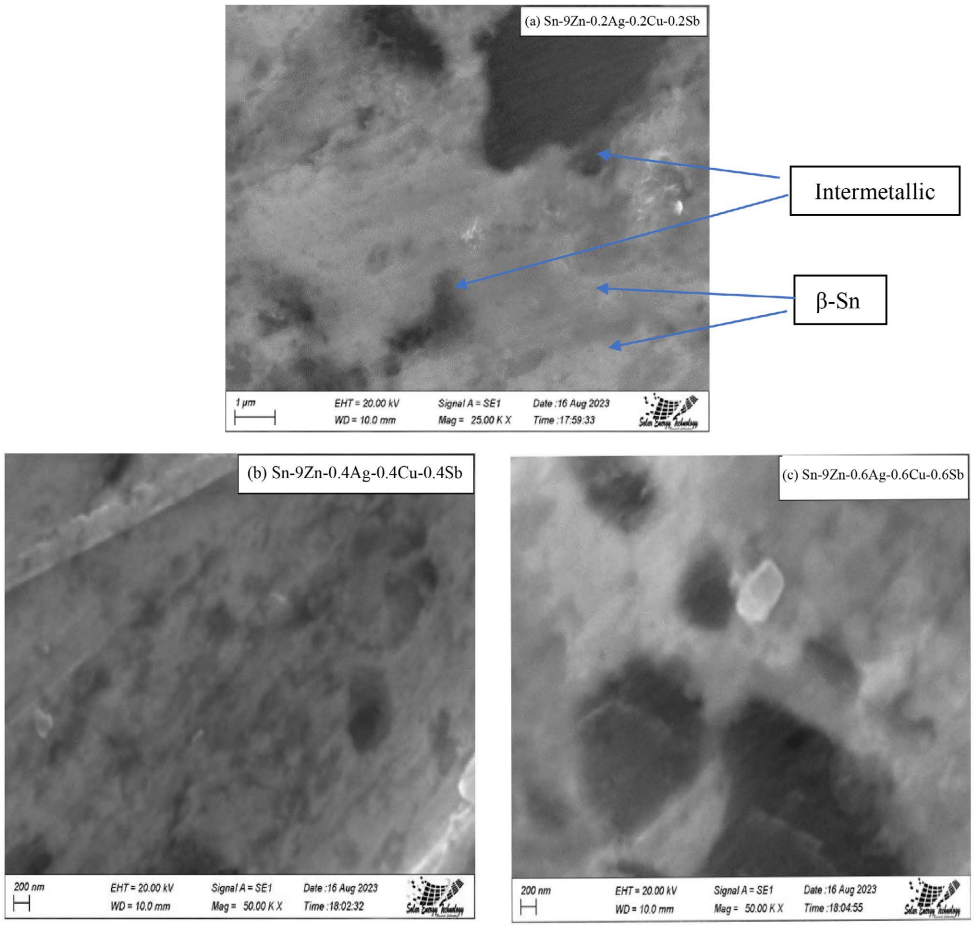

Figure 2. SEM micrograph of the quinary alloys (a) A-1 (b) A-2 (c) A-3.

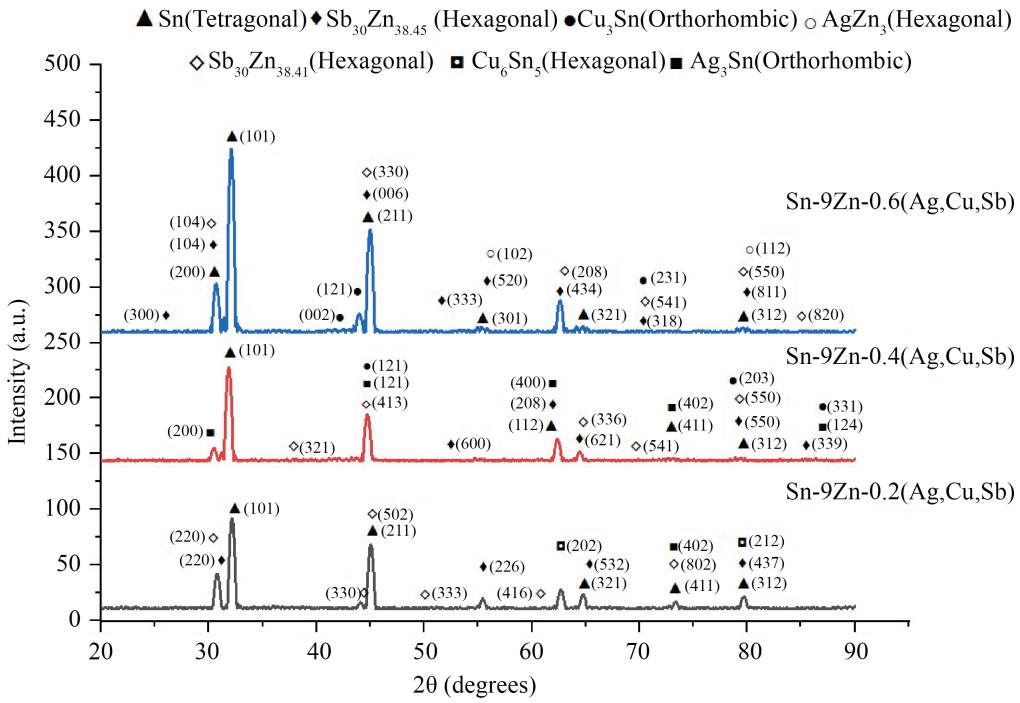

Figure 3. XRD patterns of the quinary alloys: A-1, A-2, A-3.

Moreover, alloys A-1 and A-2 have the phase Ag_3Sn (orthorhombic). Alloys A-2 and A-3 have the Cu_3Sn (orthorhombic) phase. Moreover A-1 and A-3 have the Cu_6Sn_5 (hexagonal), and $AgZn_3$ (hexagonal) phases. The intermetallic Ag_3Sn is a brittle phase with low plasticity, affecting the solder joints, mechanical properties, and thermal fatigue [44] [45]. Phases were confirmed with the analysis of the software X'Pert High Score Plus.

3.3. Microhardness

A substance's ability to withstand localized plastic deformation brought on by abrasion or mechanical indentation is measured by its hardness. The microstructure of a material influences the movement of dislocations, which in turn influences the material's hardness. A strong dependence of the Sn-based solder alloys' hardness on the alloying elements is seen [46]. The microhardness measurement can identify the microstructural variations among the alloys. The microhardness of the Sn-9Zn eutectic alloy is found to decrease when 0.2 wt% and 0.4 wt% Ag, Cu, and Sb are added (alloy A-1, A-2). But when this amount is 0.6 wt%, the hardness is increased (alloy A-3) [47]. The weak spots that developed between the complex-shaped intermetallic compounds such as $Sb_{30}Zn_{38.45}$ (hexagonal), $Sb_{30}Zn_{38.41}$ (hexagonal), Cu_6Sn_5 (hexagonal), Ag_3Sn (orthorhombic), Cu_3Sn (orthorhombic), $AgZn_3$ (hexagonal), and the matrix caused the alloys' hardness to diminish [48] [49]. The microhardness of the quinary alloys is shown in **Figure 4** with error bars. It is observed that the microhardness of the quinary alloys increases with the contents of alloying elements.

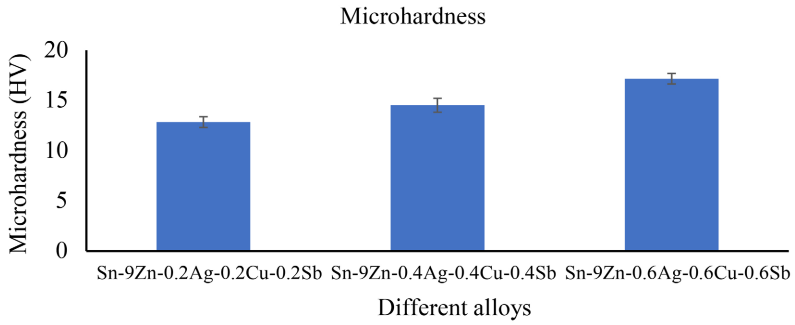

Figure 4. Vickers microhardness of the quinary alloys.

3.4. Mechanical Properties

Three types of alloys were used in the experiment. All test samples are annealed for one hour at 150˚C and an important influence is seen. The tensile test findings are summarized in Table 2, where each datum represents the average of the three samples' results. The tensile test was conducted at the strain rate of 4.17×10^{-3} s^{-1}, 20.85×10^{-3} s^{-1}, and 208.5×10^{-3} s^{-1}. Typical stress-strain curves are shown in Figure 5. Test curves for a single sample of each alloy are shown here as typical test curves; those for the other samples, which showed comparable form and appearance, are not included. It is abundantly evident that the alloying element and strain rate influence stress levels and play a significant effect. Table 2 and Figure 6 show that the ultimate tensile strength (UTS) rises as the content of alloying elements and strain rate increases over the range under investigation at room temperature. The yield strength-strain rate curves of the alloys are plotted in Figure 7. It is found that the yield strength of the alloys has a trend that is very similar to that of ultimate tensile strengths. Figure 8 displays the variation of % elongation of the different alloys. It was observed that the content of the alloying elements and strain rate for which the ultimate tensile strength is maximum, the ductility values of the alloys go through the minimum. From the

Table 2. Tensile properties of the quinary alloys.

Solder alloy	Annealing temp. and time	Strain rate ($\times 10^{-3}$ s^{-1})	UTS (MPa)	Yield stress (MPa)	Elongation (%)
(A-1) Sn-9Zn-0.2Ag-0.2Cu-0.2Sb	150˚C, 1 hour	4.17	26.10	19	60
		20.85	32.00	24.50	50
		208.5	40.38	38	41
(A-2) Sn-9Zn-0.4Ag-0.4Cu-0.4Sb	150˚C, 1 hour	4.17	27.57	21	58
		20.85	36.83	30.50	45
		208.5	48.53	44	32
(A-3) Sn-9Zn-0.6Ag-0.6Cu-0.6Sb	150˚C, 1 hour	4.17	28.97	22	44
		20.85	39.21	31	37
		208.5	52.06	45.70	34

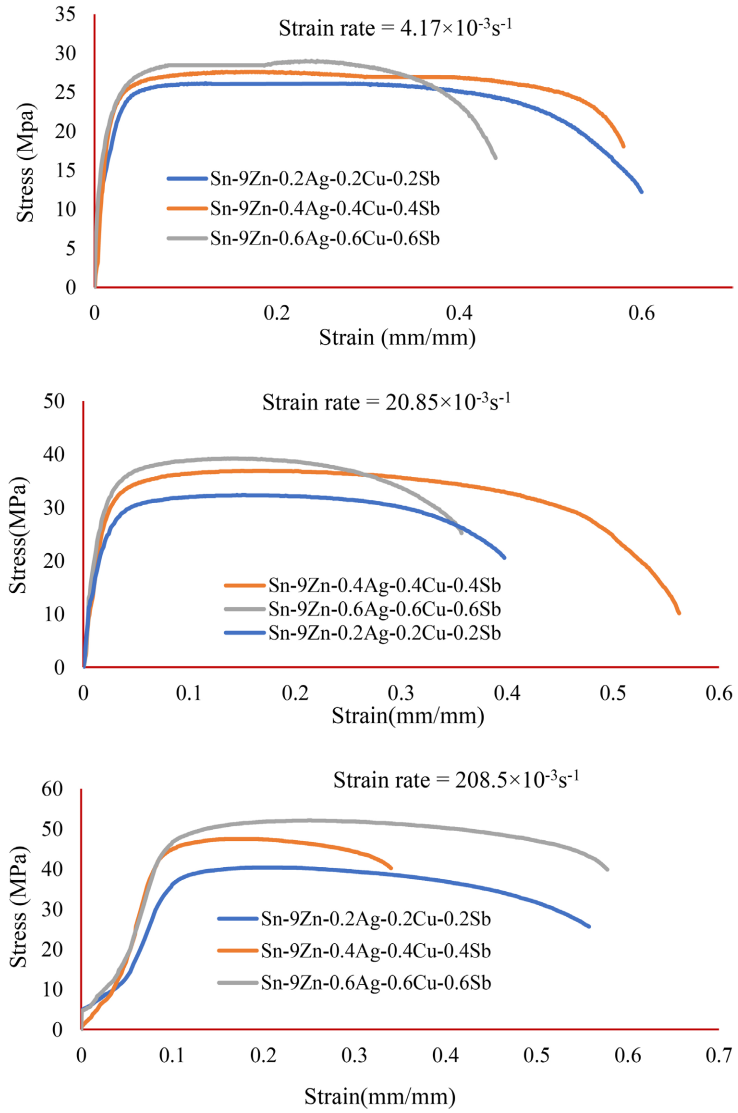

Figure 5. Typical Stress-strain curve of the quinary alloys at different strain rates.

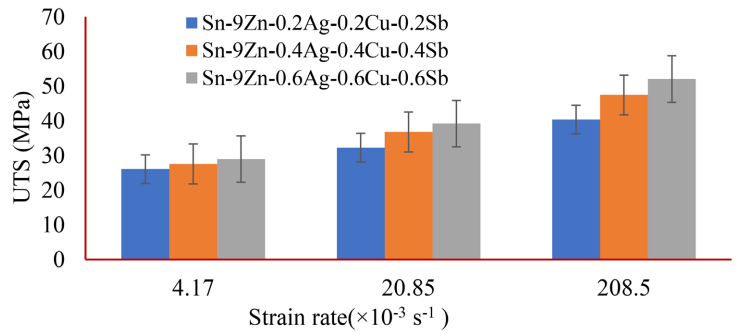

Figure 6. Average UTS values of the quinary alloys at different strain rates.

analysis of the obtained results, it is seen that the E-modulus of all the solder alloys raised with raising the content of the alloying elements as well as strain rates, which is by the previous results [50] [51] as shown in **Figure 9**.

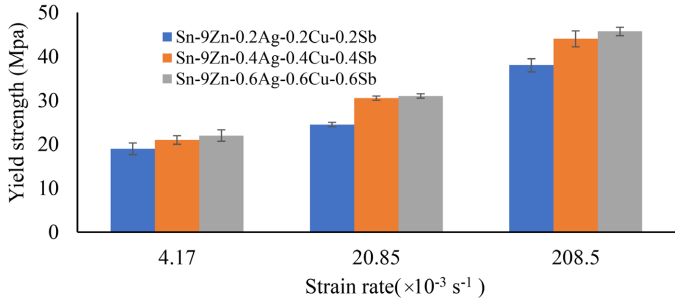

Figure 7. Average yield strength values of the quinary alloys at different strain rates.

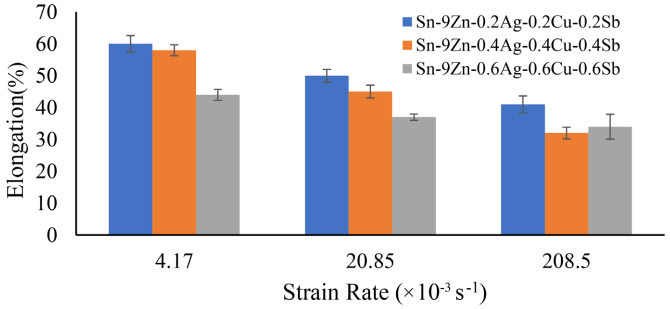

Figure 8. The ductility (%elongation) of the quinary alloys at different strain rates.

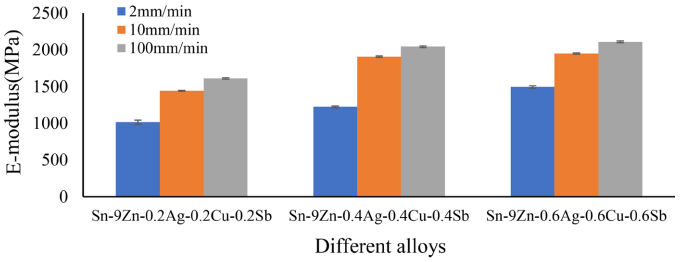

Figure 9. E-modulus of the quinary alloys at different strain rates.

3.5. Electrical Conductivity

The capacity of a material to transport an electric current is known as its electrical conductivity. Because solder alloys are used to connect circuits on printed circuit boards, their electrical conductivity is crucial. It is seen that the simultaneous addition of Ag, Cu, and Sb (quinary alloy) reduces the electrical conductivity of the Sn-9Zn alloy (**Figure 10**), increasing the solder alloys' resistivity. The initial solvent lattice structure and the additional components dissolved in the alloy are destroyed, further destroying the lattice potential field's periodicity. The alloys' electrical conductivity decreases as a result of an increase in electron scattering. Precipitation of the added components from the Sn matrix occurs when their concentration in the solder exceeds a threshold value. The precipitation delayed the electrons' travel by acting as a scattering center. Consequently, the electrical conductivity falls and the electrical resistivity rises [52] [53].

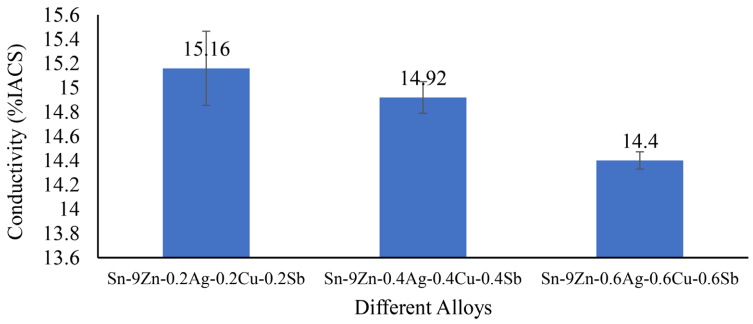

Figure 10. Electrical Conductivity of the quinary alloys.

Moreover, a drop in the number of effective electrons results from the interaction of the various complex-shaped intermetallic compounds with the additive elements, which in turn leads to a loss in electrical conductivity [54]. The conductivity of the solder connector in most microelectronics applications should be as high as possible to affect the electric circuit's functionality. The conductivity data indicate that the electrical conductivity of the Sn-9Zn and the observed alloys differs by a tiny amount.

4. Conclusions

This work aimed to replace traditional Pb-Sn solder with a lead-free Sn-9Zn eutectic solder alloy with improved characteristics. Regarding this, three quinary alloys (A-1) Sn-9Zn-0.2Ag-0.2Cu-0.2Sb, (A-2) Sn-9Zn-0.4Ag-0.4Cu-0.4Sb, and (A-3) Sn-9Zn-0.6Ag-0.6Cu-0.6Sb are prepared. The microstructure and phase analysis, microhardness testing, tensile tests, and electrical conductivity tests were performed to find out the different properties of the investigated solders. The findings led to the following conclusions:

1) It is found from the XRD examination that the β-Sn phase is formed, but there is no pure Zn phase.

2) Due to the addition of multi-alloying elements, different complex-shaped intermetallic phases formed.

3) The hardness value increased as the addition of the alloying elements Ag, Cu, and Sb increased.

4) The hardness value of the alloys A-1, and A-2 is lower compared to the Sn-9Zn eutectic alloy due to the notch effect.

5) The ultimate tensile strength (UTS) and yield strength (YS) increase, and the ductility decreases with increasing the content of alloying elements and strain rate.

6) The modulus of elasticity increases with the content of alloying elements and strain rate.

7) The nature of the yield stress is comparable to that of the UTS.

8) When the ultimate tensile strength goes through the maximum, the ductility goes through the minimum.

9) The electrical resistivity of the base alloy at room temperature was in-

creased slightly by the addition of the alloying elements due to the action of the intermetallic compounds as scattering centers for conduction electrons.

10) Studying the solder junctions' mechanical, electrical, and other characteristics is recommended.

Acknowledgments

This research work was finished with the assistance of the resources of the project titled "Establishment of Facilities for the Development of Light Engineering Sector and E-waste Processing" under the Bangladesh Council of Science and Industrial Research (BCSIR). The writers sincerely acknowledge the Prime Minister's Education Assist Trust, Bangladesh for giving the funding necessary to complete the research.

Conflicts of Interest

The authors declare no conflicts of interest regarding the publication of this paper.

References

[1] Binh, D.N. (2005) Investigations on the Properties of Sn-8Zn-3Bi Lead-Free and Sn-37Pb Eutectic Solder Alloys. Master's Thesis. http://eprints.usm.my/6555/1/INVESTIGATIONS_ON_THE_PROPERTIES_OF_Sn-8Zn-3Bi_LEAD-FREE.pdf

[2] Mishra, P. (2014) Determination and Characterisation of Lead Free Solder Alloys. Master's Thesis, National Institute of Technology Rourkela.

[3] Collins, M.N., Punch, J., Coyle, R., Reid, M., Popowich, R., Read, P., *et al*. (2011) Thermal Fatigue and Failure Analysis of SnAgCu Solder Alloys with Minor Pb Additions. *IEEE Transactions on Components, Packaging and Manufacturing Technology*, **1**, 1594-1600. https://doi.org/10.1109/TCPMT.2011.2150223

[4] Ramli, M.I.I., Saud, N., Salleh, M.A.A.M., Derman, M.N. and Said, R.M. (2016) Effect of TiO_2 Additions on Sn-0.7Cu-0.05Ni Lead-Free Composite Solder. *Microelectronics Reliability*, **65**, 255-264. https://doi.org/10.1016/j.microrel.2016.08.011

[5] Islam, R.A., Chan, Y.C., Jillek, W. and Islam, S. (2006) Comparative Study of Wetting Behavior and Mechanical Properties (Microhardness) of Sn-Zn and Sn-Pb Solders. *Microelectronics Journal*, **37**, 705-713. https://doi.org/10.1016/j.mejo.2005.12.010

[6] Chen, W.X., Xue, S.B., Wang, H. and Hu, Y.H. (2010) Reliability Studies of Sn–9Zn/Cu and Sn–9Zn–0.3 Ag/Cu Soldered Joints with Aging Treatment. *Journal of Materials Science: Materials in Electronics*, **21**, 779-786. https://doi.org/10.1007/s10854-009-9993-1

[7] Cheng, S., Huang, C.M. and Pecht, M. (2017) A Review of Lead-Free Solders for Electronics Applications. *Microelectronics Reliability*, **75**, 77-95. https://doi.org/10.1016/j.microrel.2017.06.016

[8] Union European (2003) 95/EC of the European Parliament and of the Council of 27 January 2003 on the Restriction of the Use of Certain Hazardous Substances in Electrical and Electronic Equipment. *Official Journal of the European Union*, **37**, 19-23.

[9] Collins, M. N., Punch, J. and Coyle, R. (2012) Surface Finish Effect on Reliability of SAC 305 Soldered Chip Resistors. *Soldering & Surface Mount Technology*, **24**, 240-248. https://doi.org/10.1108/09540911211262520

[10] Liu, L.J., Wu, P. and Zhou, W. (2014) Effects of Cu on the Interfacial Reactions Between Sn-8Zn-3Bi-xCu Solders and Cu Substrate. *Microelectronics Reliability*, **54**, 259-264. http://Dx.Doi.Org/10.1016/J.Microrel.2013.10.001

[11] EL-Daly, A.A. and Hammond, A.E. (2011) Development of High Strength Sn-0.7Cu Solders with the Addition of Small Amount of Ag and In. *Journal of Alloys and Compounds*, **509**, 8554-8560. https://doi.org/10.1016/j.jallcom.2011.05.119

[12] Hayes, S.M., Chawla, N. and Frear, D.R. (2009) Interfacial Fracture Toughness of Pb-Free Solders. *Microelectronics Reliability*, **49**, 269-287. https://doi.org/10.1016/j.microrel.2008.11.004

[13] (2016) Directive 2002/95/EC of the European Parliament and the Council. https://eur-lex.europa.eu/LexUriServ/LexUriServ.do?uri=OJ:L:2012:197:0038:0071:en:PDF

[14] (2016) Act for Resource Recycling of Electrical and Electronic Equipment and Vehicles.

https://www.env.go.jp/en/recycle/asian_net/Country_Information/Law_N_Regulation/Korea/Korea_RoHS_ELV_April_2007_EcoFrontier.pdf

[15] (2016) Turkey Announces RoHS Legislation. https://getenviropass.com/turkey-rohs/

[16] State Council of the Chinese Government Decree (2016) Management Methods for Restriction of the Use of Hazardous Substances in Electrical and Electronic Products. http://www.chinarohs.com

[17] J-Moss Administration Office (2016) J-Moss (Japanese RoHS). http://home.jeita.or.jp/eps/jmoss_en.htm

[18] (2016) Restrictions on the Use of Certain Hazardous Substances (RoHS) in Electronic Devices. https://www.dtsc.ca.gov/restrictions-on-the-use-of-certain-hazardous-substances-rohs-in-electronic-devices

[19] Abtew, M. and Selvaduray, G. (2000) Lead-Free Solders in Microelectronics. *Materials Science & Engineering: R: Reports*, **27**, 95-141.

[20] Li, C.J., Yan, Y.F., Gao, T.T. and Xu, G.D. (2020) The Microstructure, Thermal, and Mechanical Properties of Sn-3.0Ag-0.5Cu-XSb High-Temperature Lead-Free Solder. *Materials*, **13**, Article 4443. https://doi.org/10.3390/ma13194443

[21] Fouzder, T., Gain, A.K. and Chan, D.K. (2017) Microstructure, Wetting Characteristics and Hardness of Tin-Bismuth-Silver (Sn-Bi-Ag) Solders on Silver (Ag)-Surface Finished Copper (Cu) Substrates. *Journal of Materials Science: Materials in Electronics*, **28**, 16921-16931. https://doi.org/10.1007/s10854-017-7611-1

[22] Fima, P., Gancarz, T. Pstrus´, J. and Sypien, A. (2012) Wetting of Sn-Zn-XIn (x= 0.5, 1.0, 1.5wt%) Alloys on Cu and Ni Substrates. *Journal of Materials Engineering and Performance*, **21**, 595-598. https://doi.org/10.1007/s11665-012-0124-4

[23] Ventura, T., Terzi, S., Rappaz, M. and Dahle, A.K. (2011) Effects of Solidification Kinetics on Microstructure Formation in Binary Sn-Cu Solder Alloys. *Acta Materialia*, **59**, 1651-1658. https://doi.org/10.1016/j.actamat.2010.11.032

[24] Ren, G. and Collins, M.N. (2017) The Effects of Antimony Additions on Microstructures, Thermal and Mechanical Properties of Sn-8Zn-3Bi Alloys. *Materials & Design*, **119**, 133-140. https://doi.org/10.1016/j.matdes.2017.01.061

[25] El-Daly, A.A., Swilem, Y., Makled, M.H., El-Shaarawy, M.G. and Abdraboh, A.M. Thermal and Mechanical Properties of Sn–Zn–Bi Lead-Free Solder Alloys. *Journal of Alloys and Compounds*, **484**, 134-142.

[26] Das, S.K., Sharif, A., Chan, Y.C., Wong, N.B. and Yung, W.K.C. (2009) Influence of Small Amount of Al and Cu on the Microstructure, Microhardness and Tensile Properties of Sn-9Zn Binary Eutectic Solder Alloy. *Journal of Alloys and Compounds*, **481**, 167-172. https://doi.org/10.1016/j.jallcom.2009.03.017

[27] Silva, B.L. and Spinellib, J.E. (2018) Correlations of Microstructure and Mechanical Properties of the Ternary Sn-9wt%Zn-2wt%Cu Solder Alloy. *Materials Research*, **21**, E20170877. https://doi.org/10.1590/1980-5373-mr-2017-0877

[28] AL-ALbawee, A. (2020) Development of Sn-9Zn Solder Alloy by Adding Bismuth, Diyala. *Journal of Engineering Sciences*, **13**, 37-43. https://doi.org/10.24237/djes.2020.13405

[29] Shalaby, R.M. (2012) Effect of Silicon Addition on Mechanical and Electrical Properties of Sn-Zn Based Alloys Rapidly Quenched from Melt. *Materials Science and Engineering*: *A*, **550**, 112-117. https://doi.org/10.1016/j.msea.2012.04.041

[30] EL-Daly, A.A. and Hammand, A.E. (2010) Elastic Properties and Thermal Behavior of Sn-Zn Based Lead-Free Solder Alloys. *Journal of Alloys and Compounds*, **505**, 793-800. https://doi.org/10.1016/j.jallcom.2010.06.142

[31] Huang, H.-Z., Wei, X.-Q., Tan, D.-Q. and Zhou, L. (2013) Effects of Phosphorus Addition on the Properties of Sn-9Zn Lead-Free Solder Alloy. *International Journal of Minerals*, *Metallurgy*, *and Materials*, **20**, 563-567. https://doi.org/10.1007/s12613-013-0766-8

[32] Hu, Y.-H., Xue, S.-B., Wang, H., Ye, H. Xiao, Z.-X. and Gao, L.-L. (2011) Effects of Rare Earth Element Nd on the Solderability and Microstructure of Sn-Zn Lead-Free Solder. *Journal of Materials Science*: *Materials in Electronics*, **22**, 481-487. https://doi.org/10.1007/s10854-010-0163-2

[33] Huang, H.Z., Huang, Q.S., Peng, S. and Zhou, L. (2010) Effects of Ag Addition on Properties of Sn-9Zn Lead-Free Solder Alloys. *Rare Metal Materials and Engineering*, **39**, 1702-1706. https://doi.org/10.1016/S1875-5372(10)60127-0

[34] Chen, X., Hu, A.M., Li, M. and Mao, D.L. (2008) Study on the Properties of Sn-9Zn-XCr Lead-Free Solder. *Journal of Alloys and Compounds*, **460**, 478-484. https://doi.org/10.1016/j.jallcom.2007.05.087

[35] Billah, M.M. and Shorowordi, K.M. (2012) Effect of Micron Size Ni Particle Addition on Microstructure, Thermal and Mechanical Properties of Sn-9Zn Lead-Free Solder Alloy. *Applied Mechanics and Materials*, **229-231**, 271-275. https://doi.org/10.4028/www.scientific.net/AMM.229-231.271

[36] Gancarz, T. (2016) Physical, Thermal, Mechanical Properties and Microstructural Characterization of Sn-9Zn-XGa Alloys. *Metallurgical and Materials Transactions A*, **47**, 326-333. https://doi.org/10.1007/s11661-015-3235-3

[37] Esener, P.A., Demirel, B. and Aksöz, S. (2023) Effect of Sb and in Additives on Thermal and Electrical Properties of Sn-9Zn-4Bi Alternative Lead-Free Solder Alloy. *Materials Chemistry and Physics*, **296**, Article 127223. https://doi.org/10.1016/j.matchemphys.2022.127223

[38] Yavuzer, B., Özyürek, D. and Tunçay, T. (2020) Microstructure and Mechanical Properties of Sn-9Zn-XAl and Sn-9Zn-XCu Lead-Free Solder Alloys. *Materials Science-Poland*, **38**, 34-40. https://doi.org/10.2478/msp-2020-0025

[39] Wadud, M.A., Gafur, M.A., Qadir, M.R. and Rahman, M.O. (2015) Thermal and Electrical Properties of Sn-Zn-Bi Ternary Soldering Alloys. *Materials Sciences and*

Applications, **6**, 1008-1013. https://doi.org/10.4236/msa.2015.611100

[40] Wang, H., Xue, S.B., Zhao, F. and Chen, W.X. Effects of Ga, Al, Ag, and Ce Multi-Additions on the Wetting Characteristics of Sn-9Zn Lead-Free Solder. *Rare Metals*, **28**, 600-605. https://doi.org/10.1007/s12598-009-0115-2

[41] Wang, H., Xue, S.B., Chen, W.X. and Zhao, F. Effects of Ga–Ag, Ga–Al and Al–Ag Additions on the Wetting Characteristics of Sn–9Zn-X-Y Lead-Free Solders. *Journal of Materials Science*: *Materials in Electronics*, **20**, 1239-1246. https://doi.org/10.1007/s10854-009-9859-6

[42] Zhang, J.X., Xue, S.B., Xue, P. and Liu, S. Thermodynamic Reaction Mechanism of the Intermetallic Compounds of Sn_xNd_y and Ga_xNd_y in Soldered Joint of Sn-9Zn-1Ga-0.5Nd. *Journal of Materials Science*: *Materials in Electronics*, **26**, 3064-3068. https://doi.org/10.1007/s10854-015-2798-5

[43] Technofour Conductivity Meter Type 979. https://5.imimg.com/data5/SD/UG/HR/SELLER-1899117/digital-electrical-conductivity-meter-for-non-ferrous-metal.pdf

[44] Chen, B.L. and Li, G.Y. (2004) Influence of Sb on IMC Growth in Sn-Ag-Cu-Sb Pb-Free Solder Joints in Reflow Process. *Thin Solid Films*, **462-463**, 395-401. https://doi.org/10.1016/j.tsf.2004.05.063

[45] Chen, B.L. and Li, G.Y. (2005) An Investigation of Effects of Sb on the Intermetallic Formation in Sn-3.5Ag-0.7Cu Solder Joints. *IEEE Transactions on Components, Packaging and Manufacturing Technology*, **28**, 534-541. https://doi.org/10.1109/TCAPT.2005.848573

[46] Islam, S.M.K.N., Sharif, A. and Alam, T. (2012) Intefacial Microstructure, Microhardness and Tensile Properties of Al Microparticle Doped Sn-9Zn Eutectic Pb-Free Solder Alloy for Microelectronics Applications. *Journal of Telecommunication, Electronic and Computer Engineering*, **4**, 35-39.

[47] Wadud, M.A., Gafur, M.A., Qadir, R. and Rahman, M.O. (2015) Effect of Bismuth Addition on Structure and Mechanical Properties of Tin-9Zinc Soldering Alloy. *Materials Sciences and Applications*, **6**, 792-798. https://doi.org/10.4236/msa.2015.69081

[48] Luo, T.B., Hu, A., Hu, J., Li, M. and Mao, D.L. (2012) Microstructure and Mechanical Properties of Sn-Zn-Bi-Cr Lead-Free Solder. *Microelectronics Reliability*, **52**, 585-588. https://doi.org/10.1016/j.microrel.2011.10.005

[49] Ahmed, M., Fouzder, T., Sharif, A., Gain, A.K. and Chan, Y.C. (2010) Influence of Ag Micro-Particle Additions on the Microstructure, Hardness and Tensile Properties of Sn-9Zn Binary Eutectic Solder Alloy. *Microelectronics Reliability*, **50**, 1134-1141. https://doi.org/10.1016/j.microrel.2010.03.017

[50] Che, F.X., Zhu, W.H., Poh, E.S.W., Zhang, X.W. and Zhang, X.R. (2010) The Study of Mechanical Properties of Sn-Ag-Cu Lead-Free Solders with Different Ag Contents and Ni Doping under Different Strain Rates and Temperatures. *Journal of Alloys and Compounds*, **507**, 215-224. https://doi.org/10.1016/j.jallcom.2010.07.160

[51] Long, X., He, X. and Yao, Y. (2017) An Improved Unified Creep-Plasticity Model for SnAgCu Solder under a Wide Range of Strain Rates. *Journal of Materials Science*, **52**, 6120-6137. https://doi.org/10.1007/s10853-017-0851-x

[52] Al-Ezzi, A., Al-Bawee, A., Dawood, F. and Shehab, A.A. (2014) Effect of Bismuth Addition on Physical Properties of Sn-Zn Lead-Free Solder Alloy. *Journal of Electronic Materials*, **48**, 8089-8095. https://doi.org/10.1007/s11664-019-07577-w

[53] Peng, Y.Z., Li, C.J., *et al*. (2021) Effects of Bismuth on the Microstructure, Properties, and Interfacial Reaction Layers of Sn-9Zn-XBi Solders. *Metals*, **11**, Article 538.

https://doi.org/10.3390/met11040538

[54] Kamal, M. and Gouda, E.S. (2006) Enhancement of Solder Properties of Sn-9Zn Lead-Free Solder Alloy. *Crystal Research and Technology*, **41**, 1210-1213. https://doi.org/10.1002/crat.200610751